

The study of bronze statuettes with the help of neutron-imaging techniques

R. Van Langh · E. Lehmann · S. Hartmann ·
A. Kaestner · F. Scholten

Received: 31 May 2009 / Revised: 7 August 2009 / Accepted: 11 August 2009 / Published online: 11 September 2009
© The Author(s) 2009. This article is published with open access at Springerlink.com

Abstract Until recently fabrication techniques of Renaissance bronzes have been studied only with the naked eye, microscopically, videoscopically and with X-radiography. These techniques provide information on production techniques, yet much important detail remains unclear. As part of an interdisciplinary study of Renaissance bronzes undertaken by the Rijksmuseum Amsterdam, neutron-imaging techniques have been applied with the aim of obtaining a better understanding of bronze workmanship during the Renaissance period. Therefore, an explanation of the fabrication techniques is given to better understand the data collected by these neutron-imaging techniques. The data was used for tomography studies, which reveal hidden aspects that could not at all or scarcely be seen using X-radiography. For this specific study, the representative bronze ‘Hercules Pomarius’ of Willem van Tetrode (ca 1520–1588) has been examined, along with 20 other Renaissance bronzes from the Rijksmuseum collection.

Keywords Archaeometry · Neutron tomography · Radiography · Non-destructive testing · Fabrication process · Renaissance bronze

R. Van Langh (✉)
Department of Materials Science, Faculty 3mE,
Delft University of Technology,
Mekelweg 2,
2628 CD Delft, The Netherlands
e-mail: r.van.langh@rijksmuseum.nl

R. Van Langh · F. Scholten
Rijksmuseum Amsterdam,
PO Box 74888, 1070 DN Amsterdam, The Netherlands

E. Lehmann · S. Hartmann · A. Kaestner
Deptm. Spallation Neutron Source, Paul Scherrer Institut,
Villigen, Switzerland

Introduction

The Rijksmuseum possesses a collection of Renaissance bronze sculptures that have an important place in the collection of the museum. As a result of interdisciplinary studies between art history, conservation of art work and materials science, the interest in the fabrication techniques of these bronze statuettes has grown immensely over the years. Various technical studies have taken place resulting in catalogues and exhibitions on this interesting subject [1–5]. The study of bronze statuettes has to be performed in a non-destructive way, since sampling is impossible because of the high appreciation of the surface of these bronzes. Therefore, the research used to be limited to visual observations: with the naked eye and microscope, videoscope (only possible if there is a hole in the sculpture of minimum 4 mm) and the use of X-radiography. Neutron-imaging has proven to be an alternative tool for non-destructive investigation, and one that is complementary to common X-ray techniques [6, 7]. This is of particular importance for metals, where the penetration of neutrons in general is higher than X-rays can provide. In cases where lead, bismuth, gold or silver is involved in thicker layers, neutron imaging is usually a better tool for transmission investigations. Unlike X-radiographs, neutron imaging clearly shows hydrogenous materials like resins, core materials used for bronze casting, adhesives, wax and lacquer. Therefore, it is possible to identify visualise such materials through the thick metallic layers.

In previous years, advanced neutron-imaging techniques have been used, which are all based on digital detection systems [6, 7]. Neutron tomography can be used in addition to X-ray tomography to observe three-dimensional objects. Currently, 20 Renaissance bronze statuettes belonging to the Rijksmuseum have been examined using this technique [8], yet a comparative study using neutron tomographs and X-radiographs to evaluate the fabrication technique has not

been established. In this paper, we present the results of such an examination on Willem van Tetrode's (1520/25–1588) 'Hercules Pomarius' (Fig. 1). The research is a comparative study of various parts of the sculpture, using X-radiography, neutron radiography and neutron tomography. Neutron tomography proved useful in qualitative analysis. However, more research is needed in order to use neutron transmission as a quantitative method of analysis; for example, identifying the specific attenuation coefficients for various materials used in sculpture fabrication.

X-radiography vs. neutron radiography

Two different X-radiography methods were used in this study. The first is film-based equipment frequently used in museums



Fig. 1 Front view (a) of Hercules Pomarius by Willem van Tetrode, (BK-1954-43) with detail (b) of his face. The object is approximately 39 cm high

using an X-ray tube with an energy of 320 keV/10 mA. The drawback of this technique is the uncertainty that the picture is the optimum that can be achieved since no beam hardening correction can take place. The second is a customised GE SEIFERT DP435 digital X-ray system using a 280 keV tube at 8 mA, equipped with a metal–ceramic intensifier with an integrated high-resolution CCD camera. This setup is preferable to the film-based method since a live image of the sculpture can be adjusted and images can be recorded with both a continuous variable amperage and kilo electronvolts. However, both methods have the same drawback—usually more than one image is required in order to obtain a complete overview of a sculpture in which different metal thicknesses are present.

It is well known that X-rays interact with the electrons in the atomic shell, whereas neutrons only “see” the nuclei, ignoring the electrons completely. Therefore, the interaction probability and therefore the attenuation of X-rays rise with increasing densities. This does not hold for neutron interactions in the same way: there is no direct relationship between atomic weight and transmission. Usually, metals found in Renaissance bronzes (for example Cu, Sn, Pb) have lower attenuation values for neutrons and thus can be penetrated better with neutrons than with X-rays. On the other hand, hydrogen-containing materials such as resin, wax and sometimes also the casting core show high attenuation values with neutron radiography and can be more easily distinguished from the metals in a neutron radiograph [9].

The transmission through an object with thickness d can be described by the general attenuation law between the beam intensities in front of and behind the object, I_0 and I , respectively.

$$I_0 = I \times e^{-\Sigma \times d} \quad (1)$$

- I_0 Beam intensity in front of the object
- I Beam intensity behind the object
- Σ Macroscopic cross-section [cm^{-1}] or attenuation coefficient
- d Transmission thickness [cm]

The so-called macroscopic cross-section Σ is a material property and gives a value for the strength of interaction for the particular radiation and the beam attenuation respectively. Table 1 depicts some relevant materials for Renaissance bronzes which are listed together with the attenuation coefficients for X-rays (150 keV) and thermal neutrons (25 meV). All values for the thermal neutrons are smaller than for X-rays, resulting in higher transmission in a neutron radiograph. With X-rays of high energies, which are available in some labs for material research, a little better transmission can be achieved. The use of even more powerful radioactive gamma sources (e.g., Co-60) might be possible in some cases.

Table 1 Attenuation coefficients for X-rays and thermal neutrons for some elementary metals (unit, cm^{-1})

Material	X-ray—150keV	Thermal neutrons
Cu	1.97	1.07
Fe	1.57	1.19
Sn	3.98	0.21
Pb	22.81	0.38
Zn	1.64	0.35
Ag	5.67	4.04
Au	35.94	6.23

However, the penetrable material thickness currently depends on the sensitivity, dynamic range and signal-to-noise properties of the detection system. A remaining transmission behind the object of 2% is assumed in the data provided in Table 2.

Bronze is a generic term that encompasses alloys with copper as a main constituent. The alloying elements are predominantly tin, lead or zinc (found as binary, ternary and also quaternary alloys), yet also traces of arsenic, antimony, iron, nickel and silver are found [10, 11]. The binary and ternary alloys of copper/tin–lead or copper/zinc are most common in compositions of Renaissance bronzes where the amount of copper is usually at least 85% [11]. The high attenuation of copper and the average thickness of a bronze statuette create a limitation of analyses using X-radiography. The attenuation of the alloying components can be even higher (see Table 1): for example if objects contain high amounts of lead or tin the transmission of X-rays drops dramatically and the sculpture appears more opaque in the image. Neutrons on the other hand provide improved transmission when lead or tin are involved and therefore thicker samples can be observed. This difference in transmission cannot be overcome by any kind of X-rays (high-voltage tubes, synchrotron light or gamma radiation). A neutron transmission radiograph can be obtained from three directions *X*, *Y* and *Z*. The *X* direction is the front view, the *Y* direction is a side view of the object and the *Z* direction is from the top. An example is given in Fig. 2a–c. The different grey values in the image are a result of the variety of neutron attenuations for all materials in the sculpture. Therefore, a distinction can be made between the core materials and the bronze.

The different transmission radiographs of the “Hercules Pomarius” can now be compared in Fig. 3. The neutron radiograph was obtained in two parts which were combined using the merging option in image-processing software (in this case, AnalySiS) that allows a complete image of the sculpture to be displayed. A flat field correction was done in the case of the digital neutron image, which was impossible in the X-ray film study. Therefore, the neutron-imaging method provides more information than single images produced by film and digital transmission X-radiography.

Tomography vs. radiography

The neutron transmission image of the object in Fig. 3b immediately reveals more information than can be deduced from Fig. 3a. Furthermore, from a single X-radiograph, it is impossible to determine the thickness of the metal, or to quantify the amount of material present. These options are possible using neutron tomography since the sample is rotated around the perpendicular axes in relation to the detector system over at least 180° in equal steps (Fig. 4). The projections which are produced can deliver complete information about the whole volume when a mathematical reconstruction algorithm is applied. The resulting three-dimensional distribution of the attenuation coefficients $\Sigma(x,y,z)$ is represented by numbers for each volume element (voxel). More information about the reconstruction algorithm can be obtained in [12].

The number of voxels which have to be considered depends on the detector performance. If a single projection has for example $1,024 \times 1,024$ pixels, the number of voxels is $1,024 \times 1,024 \times 1,024$. The size of the image files gathered from the complete examination of “Hercules Pomarius” is approximately 1 Gb. Advanced visualisation tools and powerful computers are needed to treat the image data further. “Hercules Pomarius” was examined along with twenty other Renaissance sculptures using the software tool VG Studio Max 2.0 [13]. Detailed cross-section images showing the different attenuations were gathered for all the sculptures, providing information for further research. It should be noted that a preliminary examination of the images shows that it is difficult to determine where small repairs have taken place using this technique. More research should be done on this topic.

There are various possibilities that tomography offers: researchers can examine the sculpture from any point of view, by virtual slicing at positions of interest through the volume. The following options are possible:

- Enhancement of surfaces with the same attenuation level
- Segmentation of volume areas with the same voxel value
- Modification of the transparency to see inner structures better
- Measurement of distances within the object

Table 2 Material layer thicknesses which can be transmitted by X-rays and neutrons, respectively, with a residual signal of 2% (in cm)

Material	X-ray—150keV	Thermal neutrons
Cu	1.99	3.66
Fe	2.49	3.29
Sn	0.98	18.63
Pb	0.17	10.29
Ag	0.69	0.97
Au	0.11	0.63

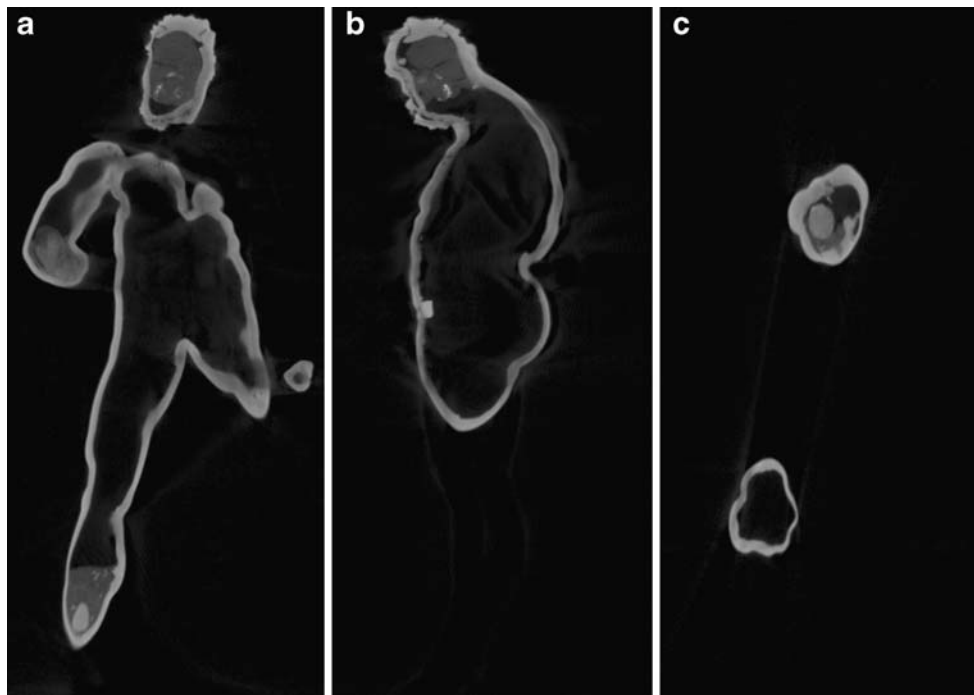


Fig. 2 **a, b, c** The images, produced by neutron radiography are two random vertical cross-sections and one horizontal cross-section of Hercules Pomarius, showing slices of the object. The images show the variety in attenuation of the materials. **a** From the *X* direction, **b** From the *Y* direction and **c** from the *Z* direction. Note in **a** at the position of the right calf, the right arm and the head have a different grey value

from the outline which corresponds to the bronze. **b** shows a different grey value in his head as well, which corresponds to the different grey value in the cross-section of the leg given in **c**. Though all of these different grey values relate to the core material it is sometimes difficult to exactly distinguish the difference between core material and bronze as can be deduced from the top image in **c**

Fig. 3 Comparison of transmission radiography with X-ray and neutron views of “Hercules Pomarius” by Willem van Tetrode. **a** Produced with X-rays at 220 keV and captured on film, **b** open-beam-corrected neutron radiography using thermal neutrons and a digital detector system. The first image was obtained at the Rijksmuseum Amsterdam and the neutron image was obtained at the NEUTRA facility, SINQ, PSI

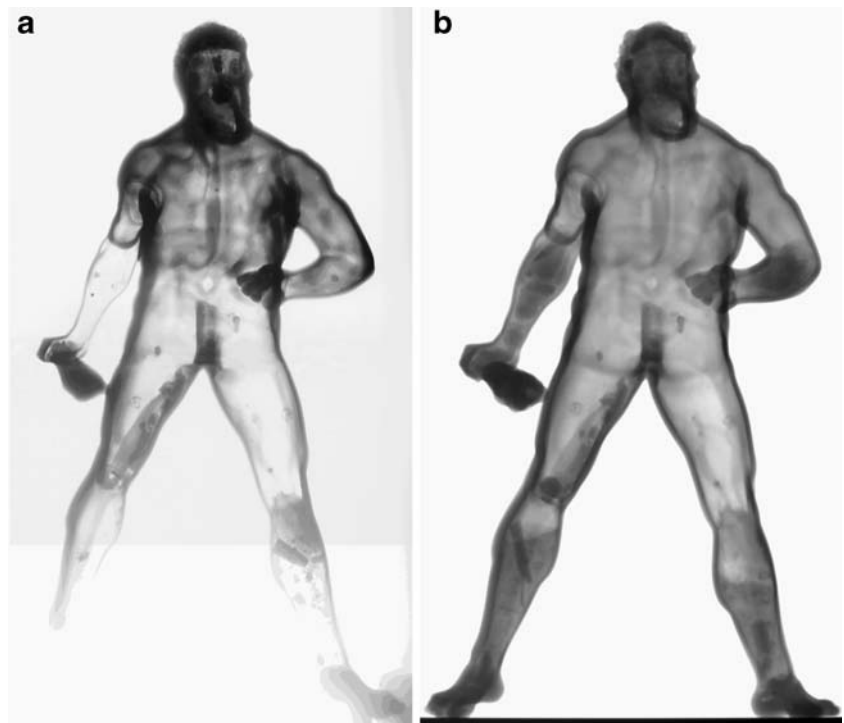
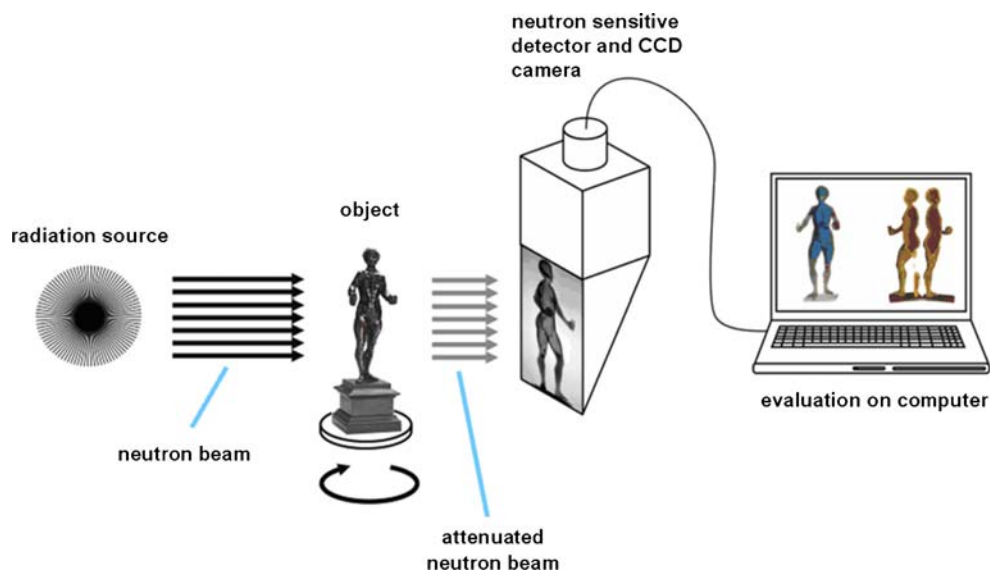


Fig. 4 Sketch of the tomography setup at PSI, based on a cooled CCD detector viewing on a neutron sensitive scintillation screen; the object is rotated around its vertical axis



- Determination of local densities, virtual “destruction” by removal of segmented regions
- Virtual moves around the object to provide a complete overview, including changes in illumination and reflection properties.

Neutron tomography facilities at PSI

The Swiss Spallation Neutron Source (SINQ) for research purposes at the Paul Scherrer Institut (PSI) is based on the principle of spallation, where high-energy protons (energy about 590 MeV, current around 1.3 mA) strike a lead target. The spallation reaction delivers about ten fast neutrons per spallation act, which are slowed down to the thermal energy (around 25 meV) in a D₂O moderator or to cold energy (around 3 meV) in a liquid D₂ moderator.

For neutron-imaging purposes, two individual facilities are available, which complement each other: NEUTRA [14] provides a well collimated and homogenous beam of thermal neutrons and ICON [15] has been built for imaging with cold neutrons. In addition, NEUTRA is equipped with a 320 keV X-ray tube (X-TRA option). For neutron tomography applications, a stationary digital neutron-imaging detection system has to be used. Although some options like amorphous silicon arrays [16] or semiconductor devices used by direct exposure in the beam are possible for tomography purposes, a cooled highly sensitive CCD camera looking via a light-reflecting mirror to a neutron sensitive scintillation screen is currently considered to be the best detection system. This setup is sketched in Fig. 2. Shown also is a rotation table, needed for turning the object around its axis, which has to be aligned perpendicular to the detector axis. Projections are recorded in regular steps from 0° to 180° (or even 360°,

depending on the divergence of the beam and the object size) with the camera detector.

The neutron-imaging stations at PSI [9] can cover a field-of-view range between 2.7 and 40 cm resulting in pixel sizes between 15 to 350 μm. The setup for micro-tomography [16] is unique in its application for highest spatial resolution.

Depending on the measurement station, measurement position, the detector system, the number of projections and the current beam intensity, a full tomography run takes between about 1 and 10 h. The optimization has to be done in respect to the final image quality needed. Since neutrons are also able to activate materials by capture, there is the potential risk for radioactivity. Table 3 shows the capture cross-sections and the half-lives of the excited isotopes for relevant structural metals. As a general rule, bronze objects will decay below the detection level within a few days of exposure.

Table 3 Activation data: excited nuclei, capture cross-sections and half-lives of excited isotopes with relevance for metallic objects, taken from [17]

Nuclide excited	Capture cross-section [barn]	Half life	Natural abundance of the target isotope [%]
Cu 64	4.5	12.7 h	69.17
Cu 66	2.17	5.1 min	30.83
Fe 59	1.3	44 days	0.28
Mn 56	13.3	2.58 h	100
Sn 121	0.13	27 h	32.59
Pb 209	0.00023	3.2 h	52.4
Ag 108	2.41	35 min	51.84
Ag 110	4.1	250 days	48.16
Au 198	98.7	2.69 days	100
Co 60	16.5	5.2 years	100
Zn 65	0.77	244.3 days	48.6

Neutron imaging (transmission radiography, tomography) is not a method that can be set up in a museum, but it can complement the common methods in cases when other methods fail or are limited. On request, the PSI's large-scale facilities (like other similar stations) are available for dedicated studies in collaboration with researchers from museums.

Quantification of the involved materials

In the ideal case, ignoring all reconstruction artefacts and uncertainties induced by scattering effects for neutrons or beam hardening effects for X-ray, the reconstructed volume consists of the attenuation coefficient in each voxel $\Sigma(x, y, z)$. In the case of a material mixture, the total value of Σ is the superposition according to (2):

$$\Sigma_{\text{tot}} = \sum_i \sigma_i \times N_i = \sum_i \sigma_i \times \frac{\rho_i \times N_A}{M_i} \quad (2)$$

Σ Macroscopic cross-section [cm^{-1}]

σ Microscopic cross-section [cm^2]

N Core density [cm^{-3}]

ρ Density [g/cm^3]

N_A Avogadro constant = 6.022×10^{23} [mol^{-1}]

M Molar mass [g/mol]

While the microscopic cross-sections are tabulated values, the material density ρ and the molar mass M are often known in advance. On the other hand, these densities might be of interest to determine, when (2) is rearranged accordingly. In the case of the "Hercules Pomarius", it was known that the outer structure is bronze, as this was previously analysed using a Bruker Artax 800 resulting in an approximate value of 80% copper and 20% zinc. The derived attenuation coefficients (macroscopic cross-sections) can then be compared to the numbers in Table 1, right column. The bronze part consists of Cu and Zn, and the resulting Σ value is dominated by Cu. The contribution of Zn to the total attenuation is significantly less.

As shown in Fig. 5, the histogram of the whole object, two peaks can be separated and attributed to bronze (in this case Cu/Zn) and the core material, respectively. The absolute numbers for the determined attenuation coefficients are however too small for both materials. Reasons might be the so-called secondary scattering in this sample as well as back-scattering effects of the neutrons, which results in smaller numbers. More effort has to be spent in the future to improve the quantitative accuracy in neutron tomography, probably by the implementation of a scattering correction algorithm (e.g. QNI [18]). Quantification can

also be made in respect to the volume of the different zones of the object. As the voxel size is well-defined by the imaging detector system setup before the tomography run, the volume of the segmented part can be calculated as the number of voxels multiplied by the voxel volume. Uncertainty is given in the segmentation when the different attenuation coefficients overlap too much.

In the case of bronze and core material for the current object (see Fig. 2c), when bronze and core material are in the same voxel the distinction between middle attenuations (core material) and high attenuation (bronze) is difficult. Based on the grey values visible in the neutron radiograph cross-sections the materials could be distinguished more easily.

Description of the object and the casting technique

Willem van Tetrode's "Hercules Pomarius" was selected as a representative Renaissance bronze to undergo neutron tomographic investigation. "Hercules Pomarius" is a sculpture depicting a defiant naked Hercules with club, holding the three golden apples of the Hesperides (Fig. 1), a reference to one of the 12 labours assigned him by King Eurystheus. The sculpture is sealed from all sides including the bottom, so videoscapy was excluded as a research technique. Because of the limitations of X-radiography as described above, neutron tomography was undertaken in the hope that it would provide evidence of fabrication techniques.

The bronze mainly consists of copper and zinc, according to analysis using X-ray fluorescence spectrometry. The bronze has a worn black patina consisting of various

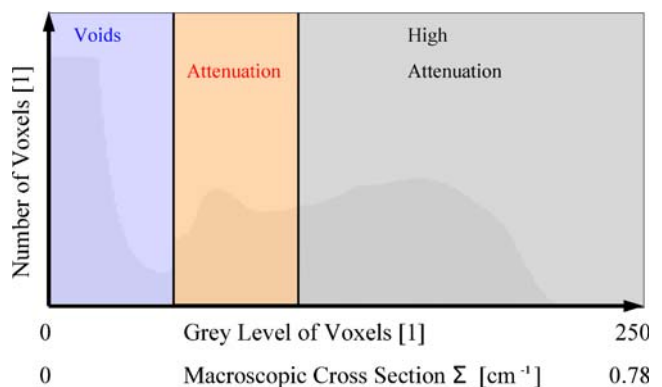


Fig. 5 The histogram of the tomography data describes the number of voxels (volume elements in the three-dimensional data set, unit integer values) with a particular grey level. The macroscopic cross-sections can be obtained by a linear scaling factor. Note the line between middle and high attenuation. Since the number of voxels changes very gradually here, it is very difficult to distinguish between the attenuations

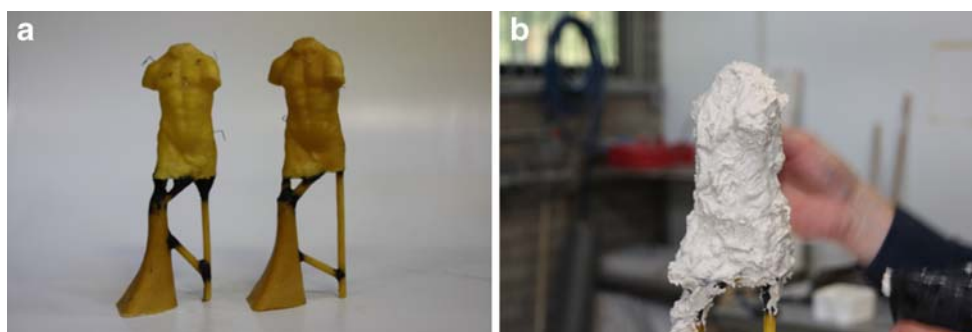


Fig. 6 Schematic overview of the preparation of lost wax casting, **a** the wax prepared with ingot (v-shaped), and rod where the iron core pins are put in the wax, **b** the first and second fire-proof layers are applied, **c** to hold the outer core in place, chicken wire is used to

strengthen the shape (any shape) while the figure is now partially surrounded by coarse grains of the outer core that will fill up the complete figure

beeswax components and other organic materials as indicated by direct temperature-resolved mass spectrometry on two samples (DTMS).

During the Renaissance there was one technique in use for casting hollow bronzes: lost wax casting, which is based on the principal that all wax in a model is to be replaced by bronze. Bewer [11] has extensively reported on the methods used during the Renaissance period. Lost wax casting can be subdivided in two techniques: a direct method, when an object is made of which the original model is lost, and an indirect method, when the original model survives the process. It is important to understand the difference since neutron tomography offers the opportunity to determine which technique has been used.

Direct method

This method starts with a wire skeleton covered with a core of fire-proof material such as clay or plaster that forms the rough shape of the final sculpture. This fire-proof rough model, also called the ‘inner core’, is covered with a thin and even wax layer with a thickness between 3–6 mm depending on the size of the object and which is finished according to the sculptor’s

desire. The resulting wax model filled with core material gives the impression of what the final sculpture will look like when the wax is replaced by bronze. Iron pins are inserted through the wax into the core material and protrude visibly. A large wax ingot is mounted and, depending on the size of the sculpture, wax rods are applied to function as vents that will distribute the metal to all openings within the mould, or free the entrapped gas that may arise (Fig. 6a). Subsequently, the wax is covered with a wetting agent such as ox-gall and spread with a watery mixture of powdered fire-proof material similar to the inner core material. On top of this first layer, a second layer of the same material with coarser grains is put on, almost covering the iron pins as well (Fig. 6b). Finally, all is covered with a thick layer of the same fire-proof material. The mixture of all layers on top of the wax is subsequently called the ‘outer mould’. The complete mould is heated in an oven, and all the wax melts out through the rods and the ingot. At this moment, the inner and outer cores are held in place by the iron pins. The structure is inverted and molten metal is poured into the open space between the inner and outer core through the open space left by the ingot. Once the empty space between both cores is filled with molten metal, it will rise through and eventually begin to flow out of the space left by the rod.

Fig. 7 Captured images of Hercules Pomarius from a live view. Indicated in red are the cracks in the hair which do not appear to go fully through. These images were captured at 198 keV/1.1 mA

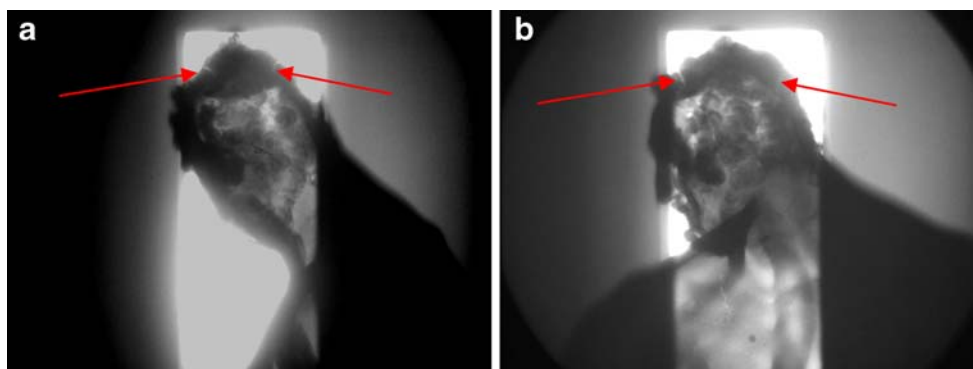


Fig. 8 Reconstructed neutron tomography of Hercules Pomarius. The *grey colour* in this image represents the bronze, the *yellow colour* represents the core material. Both colours are added by software manipulation

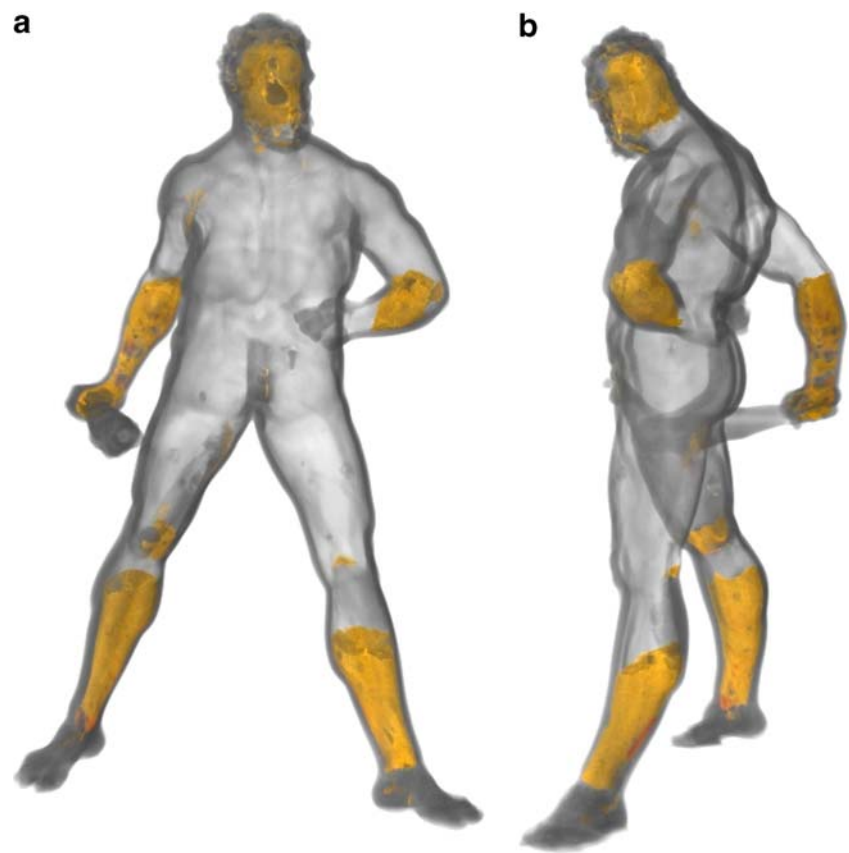


Fig. 9 Images from both the *X* (a) and *Y* (b/c) direction indicate that at the top of his head, there is a clear fissure running completely through the bronze. Also note the distinct *medium-grey feature* showing extra bronze at the height of the nose in image c



Indirect method

This method is different from the direct method since no metal skeleton is preformed to the shape of the sculpture; an existing model is used instead to take an imprint. The original material can be bronze, terra cotta, wood or any other material. The imprint is usually made of plaster, and depending on how many undercuts a sculpture would have, piece-moulding would have to take place [11]. After the mould making, the plaster sections of the mould are soaked in water and put together, providing a negative form of the model. There are various methods for putting the wax layer in; one is to pour hot wax into the mould, slush it around and to decant, leaving a thin layer of wax behind. By doing this repeatedly, a build-up of layers can be formed to any desired thickness, usually between 3–6 mm. The wax model is taken out of the (piece)mould and is filled and covered with fire-proof material as with the direct method. Subsequently, the whole casting procedure follows the direct method.

Finishing

Both methods result in a rough sculpture with sprues and vents still attached; the direct method additionally has the wire skeleton and inner core inside, while the indirect method only has the inner core material present. The excess metal is cut off, the sculpture is usually finished by chasing, and the core material is chipped away where accessible, through openings in the sculpture. For both methods, if a small chip of core material shifts or breaks off in the mould, after or during melting out the wax, this results in a casting flaw or gap in the sculpture. In such cases, repairs can be made using the technique called “casting on” or “after-casting” [19]. The technique is fairly simple: the part that failed to come out of the cast is modelled in wax again directly on the sculpture. Then, the piece is cast in place according to the direct casting method. It should be emphasised that ‘casting on’ is only done during fabrication of the object.

Results of the X-radiography

The film-based X-radiograph of “Hercules Pomarius” in Fig. 2a appears to show that there are various thicknesses of the metal in the torso and the legs since they do not show the same attenuation on the image. However, it is impossible to see whether variations in the grey scale are caused by the presence of a thick layer of core material or simply thicker metal. The legs are overexposed and do not show anything of the fabrication technique, and the proper

right forearm appears hollow. The sculpture was later examined using the current digital X-radiography setup at the Rijksmuseum Amsterdam, which provided more useful information. This technique showed peculiar cracks in the head of the sculpture—partly through the hair—as can be observed in Fig. 7. Although the cracks do not appear to go through the thickness of the metal, their presence suggests that the crown of the head could be a separate piece, meaning that the complete sculpture was not cast in one run.

Results of the neutron transmission and tomography investigation

The neutron transmission radiograph clarifies the information provided by the X-radiographs. Figure 8 shows the neutron tomography images of the sculpture, produced by manipulation of the attenuation values along the X , Y and Z axes (as clarified in Fig. 2). The reconstructed pictures clearly show the absence of core material in the torso. However, in both arms and legs, and also in the head, core material is visible.

Regarding the casting technique, if the direct method had been used, a wire skeleton should have been present, at least going into his feet. Since this is absent, we can now safely conclude that this sculpture was indirectly cast. The neutron radiographs show that most of the core



Fig. 10 Photograph of the back of the head of Hercules Pomarius corresponding to the cross-section depicted in Fig. 11a–f

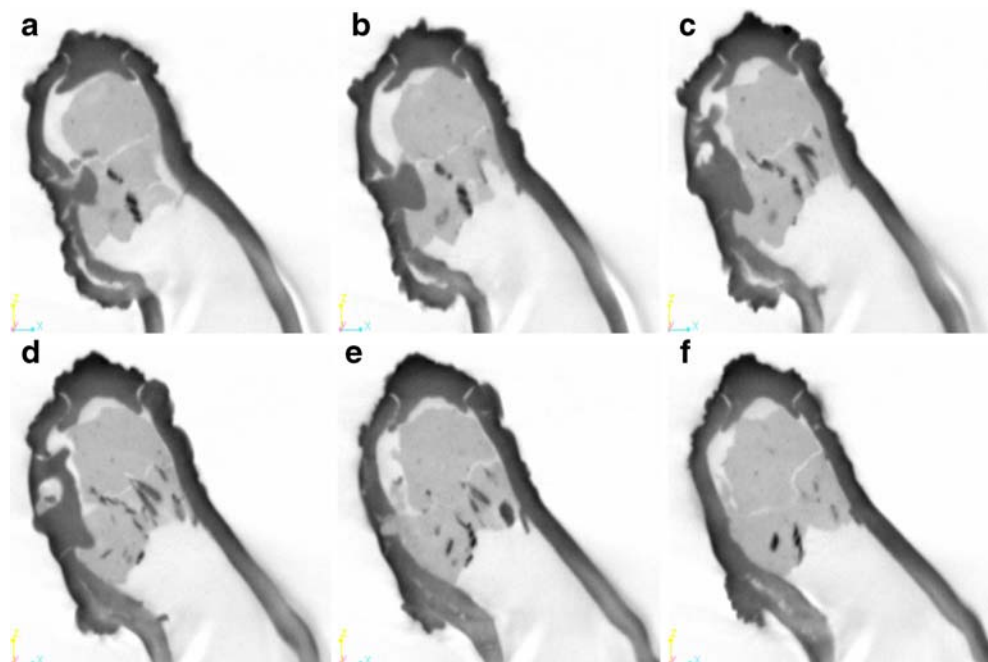
material was removed, we now need to consider how remains of the core material could have been retrieved from the sculpture, considering that the sculpture is completely closed. Figure 9a–b shows raw images from neutron radiographs on which features on the head of the sculpture can be seen.

The crack that was first seen in the digital X-radiograph (Fig. 7) is more clearly shown to be a complete crack that separates the top part of the head from the rest of the sculpture (Figs. 10 and 11a–b). The suggestion of the X-radiograph has hereby been confirmed: part of the sculpture was ‘cast on’. Furthermore, Fig. 9c shows that the space behind the nose is filled with additional bronze. A plausible explanation of this is as follows: during the casting process the inner mould was damaged at the height of the nose. A detached piece of the inner core behind the nose fell into the space where the top of the head should be. The piece therefore blocked the flow of the metal to this area, resulting in a gap at the crown of the head. Conversely, the space from which it fell (behind the nose) was filled with excess bronze. Therefore, the crown of the head had to be remodelled in wax and cast on to the finished sculpture. Furthermore, this explains how it was possible to remove most of the core material from the otherwise completely closed-off sculpture, leaving only remnants in the legs, arms and head. The core material from the body had to be removed through the (unintended) opening in the head. Then, during casting-on of the crown of the head, additional core material was placed inside the head as a support for the wax.

Conclusions

Since the attenuation of neutrons is so different from that of X-rays, neutron radiography is a good complement to conventional X-radiography for studying Renaissance bronzes especially when core materials are present, or heavier elements that cannot be easily penetrated by X-rays are present in an alloy. In the case of Hercules Pomarius, it was only through the use of neutron tomography that the fabrication techniques could be revealed. Neutron tomography is potentially a very powerful tool in the study of Renaissance bronzes, since it provides ‘real insight’ in these objects of art. Neutron tomography is a technique that should be used for studying complete oeuvres of sculptors. When used in conjunction with art, historical and technical knowledge of works of art, it will definitely change the attributions of many fine-art objects given by curators based on stylistic features alone. Therefore, it will have a great impact within the art historical community. This approach towards studying Renaissance bronzes will contribute significantly to our cultural heritage as is being recognised by major museums worldwide which are now joining together to study these beautiful objects of fine art. Finally, when fine-art objects are being chosen as a subject of scientific study fabrication, it is imperative to include the ever underestimated fabrication techniques in these kinds of studies since they provide the needed difference for understanding the results from scientific analysis on these objects of art.

Fig. 11 The sequence of pictures a–f from the Y direction showing slices at various depths covering about 10 mm in the centre of the sculpture, at the head. The images show that the crown of the head is completely separate (and therefore cast on) and an excess of bronze has formed in the space where a piece from the inner mould fell off, behind the nose



Acknowledgement The DTMS analysis were executed by Prof Dr Jaap Boon, FOM Institute for Atomic and Molecular Physics [AMOLF] Science Park 113 1098 XG Amsterdam

Open Access This article is distributed under the terms of the Creative Commons Attribution Noncommercial License which permits any noncommercial use, distribution, and reproduction in any medium, provided the original author(s) and source are credited.

References

1. Stone RE (1982) Antico and the development of bronze casting in Italy at the end of the Quattrocento. *Metrop Mus J* 16:87–116
2. Stone RE (2006) Severo Calzetta da Ravenna and the indirectly cast bronze. *Burlington Magazine* 148(1245):810–819 December
3. Stone RE. Andrea Riccio, renaissance master of Bronze, Riccio: technology and connoisseurship. Frick Collection, New York, pp 81–97
4. Scholten F, Van Binnebeke E, Bewer FG, Van der Mark B, De Koomen A. Willem van Tetrode, sculptor, Rijksmuseum Amsterdam – The Frick Collection. Waanders, New York
5. Scholten F et al (1998) Adriaen de Vries. Waanders, Zwolle 1556–1626
6. Rant J, Milič Z, Turk P, Lengar I (2005) Neutron radiography as a NDT method in archaeology, application of contemporary non-destructive testing in engineering. Portorož, Slovenia, pp 181–188 September 1-3
7. Anderson IS, McGreevy RL, Bilheux HZ. Neutron imaging and applications. Springer Science+Business Media, LLC 2209, 987-0-387-78692-6, E. Lehmann, P. Vontobel, L. Tobler, L. Berger. E. Lehmann, P. Vontobel, L. Tobler, L. Berger, E. Deschler-Erb, A. Voûte, PSI Progress Report 2002 (NUM Dept.)
8. Scholten F, Verber M, Van Langh R, Visser D (2005) From Vulcan's forge: bronzes from the Rijksmuseum Amsterdam 1450–1800. Katz, London http://www.rijksmuseum.nl/formats/startStory.jsp?id=vulcanus_11&lang=nl
9. <http://neutra.web.psi.ch/>
10. S. Christanetti et al, Recent acquisitions made to the Robert H. Smith Collection of Renaissance Bronzes, *The Burlington Magazine*, Hampshire, 2007
11. Bewer FG (1996) A study of the technology of Renaissance bronze statuettes, London, Dissertation, Dept. of Archaeological Conservation and Materials Science, University of London, University College, Institute of Archaeology
12. Banhart J (ed) (2008) Advanced tomographic methods in materials research and engineering. Oxford, pp 34
13. <http://www.volumegraphics.com/>
14. Lehmann E, Vontobel P, Wiezel L. Properties of the radiography facility NEUTRA at SINQ and its use as European reference facility. *Nondestr Test Eval* 00:100-113
15. Kühne G et al (2005) ICON—the new facility for cold neutron imaging at the Swiss spallation neutron source SINQ. *Swiss Neutron News* 28:20–29 http://sgn.web.psi.ch/sgn/snn/snn_28.pdf
16. Lehmann EH et al (2007) The micro-setup for neutron imaging: a major step forward to improve the spatial resolution. *Nucl Instrum Methods Phys Res A* 576(2-3):389–396
17. Karlsruher Nuklidkarte, Report EUR 22276 EN
18. Hassanein R (2006) Correction methods for the quantitative evaluation of thermal neutron tomography, Dissertation No. 16809, ETH Zürich, Switzerland
19. Cellini B (1982) *Het leven van Benvenuto Cellini*, tr. Van Dam van Isselt, H., Van Schendel, C., 2^e herz druk, Amsterdam, 1982, 364–367